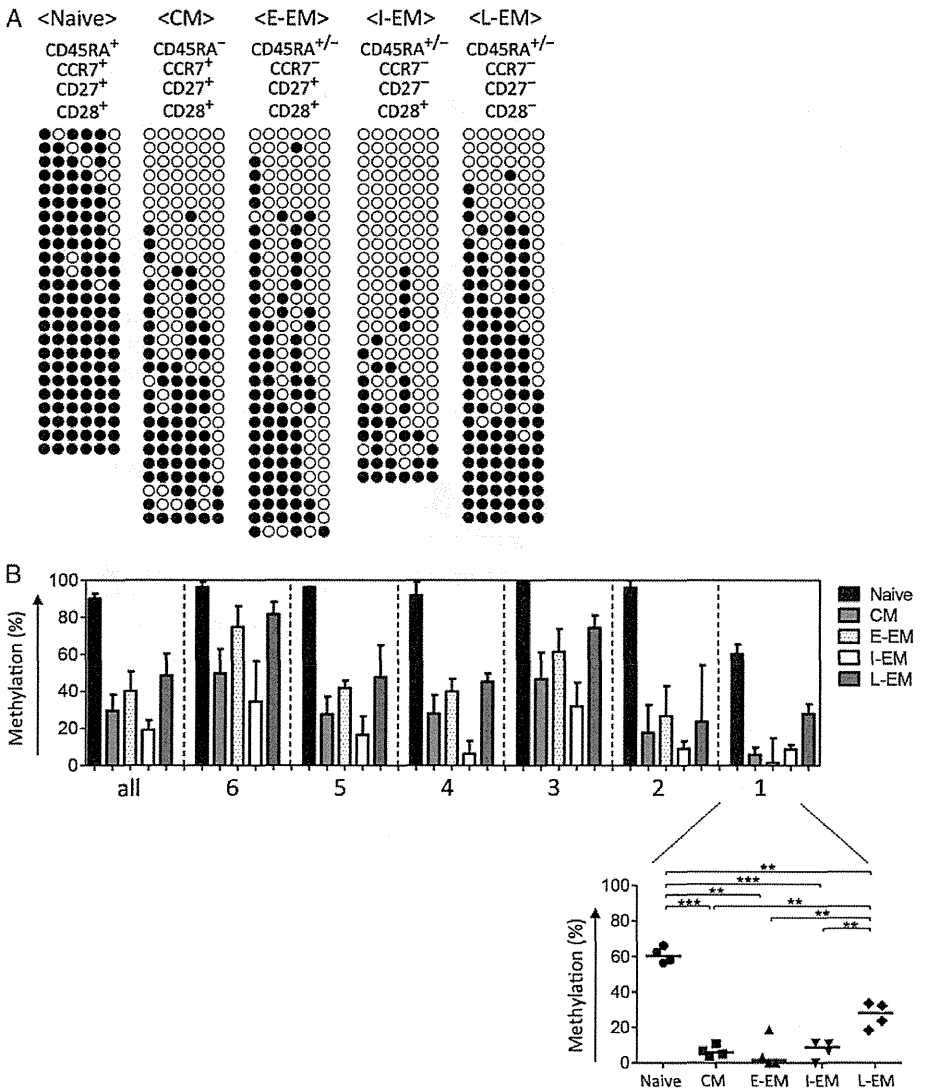

Figure 3. DNA methylation status of the *IL2* locus in different CD4+ T-cell subsets. *A*, Representative bisulfite sequencing DNA methylation analysis of the *IL2* locus in naive, central memory (CM), early effector memory (E-EM), intermediate effector memory (I-EM), and late effector memory (L-EM) CD4+ T-cell subsets, classified according to CD45RA, CCR7, CD27, and CD28 expression. *B*, Summary graph of DNA methylation status of the *IL2* locus in T-cell subsets in 4 individuals without HIV-1 infection. The paired *t* test was performed for statistical analysis. $^{**}P = .001–.01$, $^{***}P < .001$.

Phenotypically Senescent Memory CD4+ T Cells Have a Methylated *IL2* Promoter

Although the DNA methylation status of the *IL2* promoter/enhancer region in different CD4+ T cells in mice has been well characterized [17, 29, 30], the detailed profile of *IL2* promoter methylation in human CD4+ T cells has not been elucidated. Therefore, we sorted different CD4+ T-cell subsets in HIV-1-uninfected individuals on the basis of CD45RA, CCR7, CD27, and CD28 expression [31–33] and assessed the methylation status of the *IL2* promoter in each fraction (Figure 3). CpG sites 2–6 were fully methylated, and CpG site 1 was 60% methylated in naive CD4+ T cells (Figure 3*A* and 3*B*). In contrast, CpG sites 2–6 were >50% demethylated in all memory subsets (Figure 3*B*). Moreover, CpG site 1 was fully demethylated in central memory, early effector memory, and intermediate effector memory cell compartments (Figure 3*B*). Interestingly, all CpG sites, including site 1, were remethylated in late effector memory cells. Since signaling through CD28 has been shown to modify the epigenetic program of the *IL2* promoter in mice [30], we postulated that the *IL2* promoter may have an altered DNA methylation program in late effector memory subsets without CD28 expression.

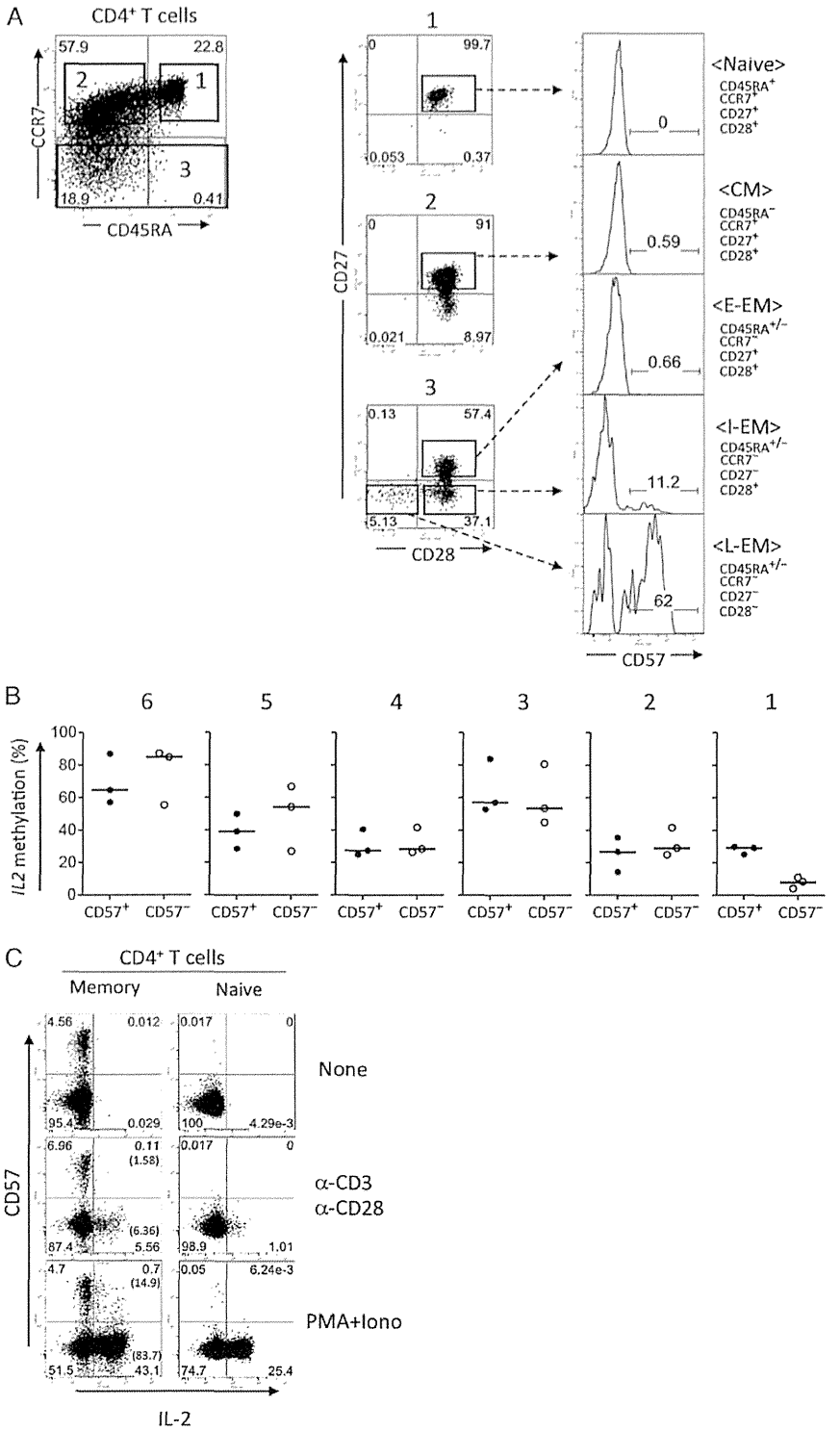

Figure 4. Analysis of CD57 expression and *IL2* locus DNA methylation in memory CD4$^+$ T-cell subsets. *A*, Representative flow cytometric analysis of CD57 expression on CD4$^+$ T-cell subsets classified by CD45RA, CCR7, CD27, and CD28 expression. *B*, Summary graph of the *IL2* locus DNA methylation status at CpG sites 1–6 in CD57$^+$ and CD57$^-$ memory (CD45RA$^-$) CD4$^+$ T cells from 3 individuals without human immunodeficiency virus type 1 (HIV-1) infection. *C*, Flow cytometric analysis of CD57 and IL-2 expression after stimulation with α-CD3/CD28 and PMA/ionomycin in peripheral blood mononuclear cells from an HIV-1-uninfected individual. Values within brackets indicate the proportion of IL-2 secreting cells in CD57$^+$ and CD57$^-$ cells. Abbreviations: CM, central memory; E-EM, early effector memory; I-EM, intermediate effector memory; L-EM, late effector memory.

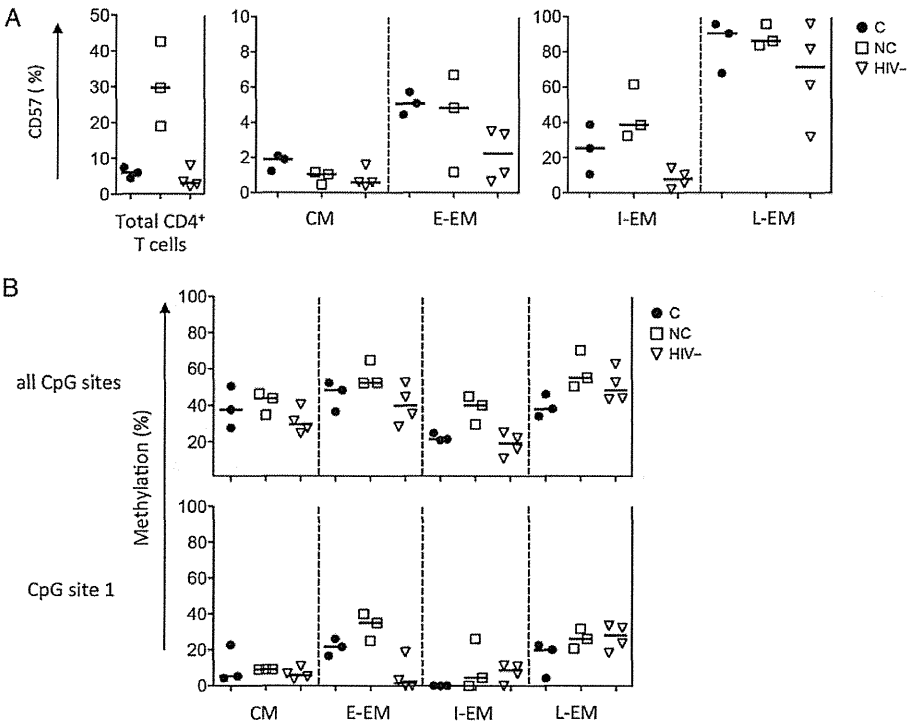

Figure 5. DNA methylation analysis of the *IL2* locus in memory CD4+ T-cell subsets from individuals with chronic human immunodeficiency virus type 1 (HIV-1) infection. Summary graphs of CD57 expression level (*A*) and DNA methylation status of the *IL2* locus (*B*) in memory CD4+ T-cell subsets. The memory subsets were defined by CD45RA, CCR7, CD27, and CD28 expression as shown in Figure 4*A*. Abbreviations: C, viremic controller; NC, noncontroller; HIV-, HIV-1-uninfected; CM, central memory; E-EM, early effector memory; I-EM, intermediate effector memory; L-EM, late effector memory.

It has also been reported that expression of CD57 is highly correlated with loss of CD28 expression in $CD4^+$ T cells [34–36] and is associated with replicative senescent T cells [34, 37, 38]. On the basis of these observations, we evaluated the association between CD57 expression and DNA methylation of the *IL2* promoter. We first analyzed CD57 expression in each $CD4^+$ T-cell subset. Naive, central memory, and early effector memory $CD4^+$ T cells from healthy individuals did not express CD57, while a significantly increased frequency of $CD4^+$ T-cell subsets with a more differentiated phenotype expressed CD57, with the highest level of expression observed on the late effector memory subset. We next assessed the DNA methylation status of the *IL2* promoter in $CD57^+$ and $CD57^-$ subsets of memory ($CD45RA^-$) $CD4^+$ T cells (Figure 4*B*). We found that CpG site 1 was more methylated in the $CD57^+$ subsets relative to the $CD57^-$ subsets. Importantly, IL-2 secretion in CD57-expressing memory $CD4^+$ T cells was 5-fold lower than IL-2 secretion in $CD57^-$ memory $CD4^+$ T cells even after strong T-cell stimulation with PMA/ionomycin (14.9% vs 83.7%; Figure 4C). These data indicate that $CD57^+$ cells among late effector memory $CD4^+$ T cells were remethylated at CpG site 1 of the *IL2* promoter, which was coupled to restricted IL-2 expression.

$CD57^+CD4^+$ T Cells in HIV-1–Infected Noncontrollers Have a Methylated *IL2* Promoter and Restricted IL-2 Expression

It has also been reported that HIV-1-specific $CD57^+CD4^+$ T cells have reduced IL-2 expression [35, 39]. Abnormal T-cell differentiation of polyclonal $CD4^+$ and $CD8^+$ T cells in HIV-1-infected individuals is associated with increased levels of CD57 expression [5, 35]. To determine whether the increased immune dysfunction in polyclonal memory T cells during chronic HIV-1 infection is associated with stable epigenetic programming of the memory pool, we measured DNA methylation of the *IL2* promoter in memory $CD4^+$ T-cell subsets from HIV-1–infected individuals. As previously reported [5, 35], the number of $CD57^+$ effector memory (early, intermediate, and late) $CD4^+$ T cells was higher in chronically infected individuals, compared with individuals without HIV infection (Figure 5*A*). We also observed an increase in methylation of the *IL2* promoter, not only in the late effector memory subset, but also in the less differentiated early effector memory and intermediate effector memory subsets from noncontrollers (Figure 5*B*). These data suggest that aberrant epigenetic modification at *IL2* promoter, coupled to CD57 expression, occurs at an early stage of $CD4^+$ T-cell differentiation during chronic HIV-1 infection.

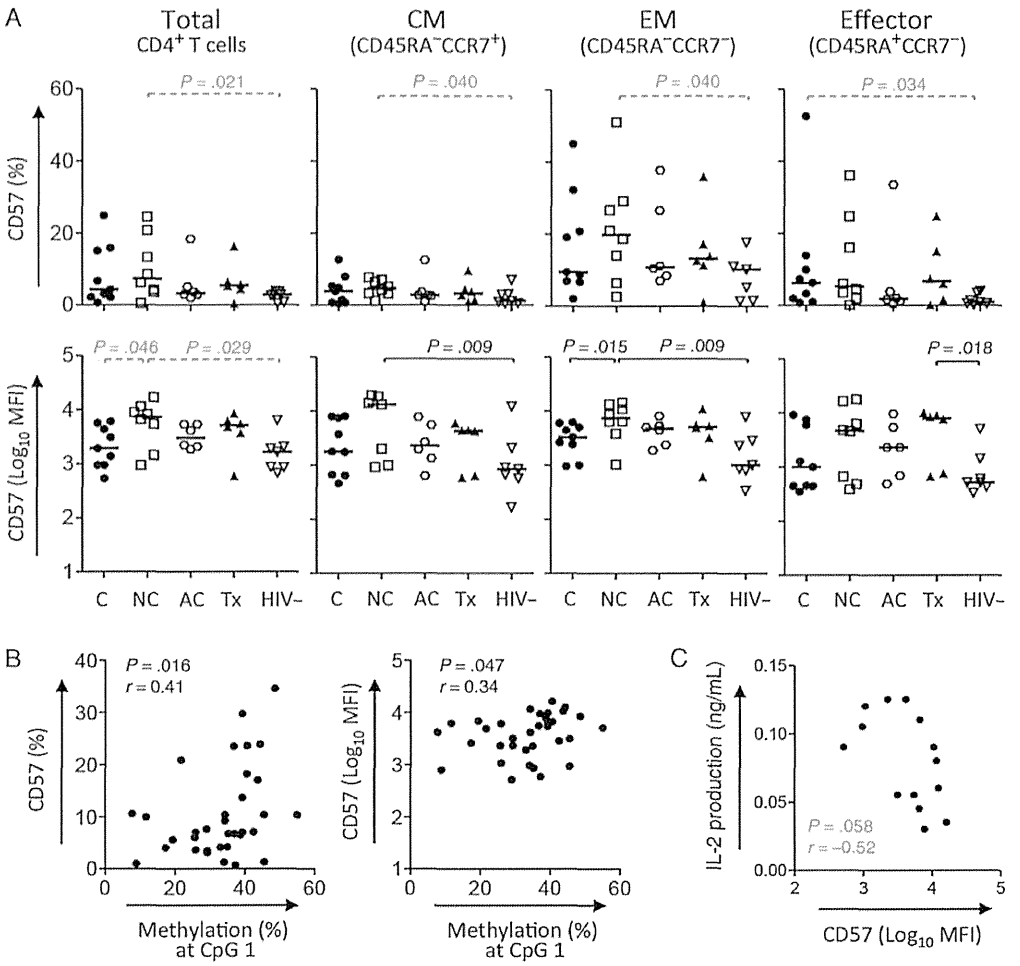

Figure 6. CD57 expression and methylation analysis of CpG site 1 in the *IL2* locus of CD4 memory T-cell subsets from individuals with human immunodeficiency virus type 1 (HIV-1) infection. *A*, Summary graph of CD57 expression level in each subset of $CD4^+$ T cells classified by CD45RA and CCR7. The Mann–Whitney *U* test was used for statistical analysis. *B*, Correlation plot of methylation at CpG site 1 vs CD57 expression in memory $CD4^+$ T cells. *C*, Correlation plot of methylation at CpG site 1 in $CD4^+$ T-cell vs IL-2 production in PHA-stimulated PBMCs. Correlation coefficient and *P* values in Spearman's rank correlation test are shown. *P* values less than .05 with $q > 0.2$ show in gray. Abbreviations: C, controller; NC, noncontroller; Ac, acute HIV-1 infection; Tx, treated with cART; HIV-, HIV-1-uninfected; CM, central memory; EM, effector memory.

We next measured the level of CD57 expression on individual $CD4^+$ T-cell subsets in all study groups (Figure 6*A*). Our data reveal that the frequency of $CD57^+$ cells was higher in noncontrollers than other groups and that the mean fluorescence intensity of CD57 expression on the total pool of memory $CD4^+$ T cells was significantly higher in noncontrollers.

Finally, we performed a correlation analysis between CD57 expression, DNA methylation of the *IL2* promoter, and IL-2 expression. A positive correlation was observed between CD57 expression and DNA methylation at CpG site 1 in the *IL2* promoter (Figure 6*B*). We also found a negative correlation between CD57 expression and IL-2 production in HIV-1–infected individuals (Figure 6*C*). Together, these data support a model whereby prolonged exposure of memory $CD4^+$ T cells to the chronic inflammatory environment in HIV-1 noncontrollers results in upregulation in CD57 expression and hypermethylation of the *IL2* promoter, ultimately resulting in senescence of polyclonal memory $CD4^+$ T cells.

DISCUSSION

Although many studies about T-cell immunopathogenesis during chronic HIV-1 infection have been reported, the molecular basis for T-cell dysfunction is not well understood. To better understand the mechanism for the broad decline in $CD4^+$ T-cell function during chronic HIV-1 infection, we performed

a combination of molecular and cellular assays that assessed the epigenetic profile of T cells relative to their ability to express cytokines in HIV-1 noncontrollers. Our results demonstrate that the CpG sites in the *IL2* promoter are highly methylated in $CD4^+$ T cells in noncontrollers and that the lower IL-2 expression is correlated with *IL2* promoter DNA methylation in $CD4^+$ T cells. Furthermore, DNA methylation was positively correlated with CD57 expression on memory $CD4^+$ T cells. To understand the relationship between $CD4^+$ T-cell quality and the *IL2* DNA methylation, we sorted $CD4^+$ T-cell subsets on the basis of differentiation and senescent markers and analyzed the methylation of CpG sites in the *IL2* locus. Naive $CD4^+$ T cells were fully methylated, and demethylation occurred at all CpG sites during T-cell differentiation, consistent with previous reports using mouse model systems [17, 19]. CpG sites were partially but significantly remethylated in terminally differentiated $CD4^+$ T cells in healthy individuals. We also found that $CD57^+$ cells, most of which possessed a terminally differentiated phenotype in HIV-uninfected individuals, were highly methylated at CpG site 1, compared with $CD57^-$ memory $CD4^+$ T cells. In contrast, the *IL2* promoter in memory $CD4^+$ T cells from HIV-1–infected noncontrollers was highly methylated. Further, the promoter was also methylated in less differentiated $CD57^+$ memory $CD4^+$ T cells. Taken together, our data suggest that loss of *IL2* expression in senescent $CD4^+$ T cells is regulated by DNA methylation during chronic HIV-1 infection.

Our results indicate that the genomic region proximal to CpG site 1 in the *IL2* promoter is important for transcriptional regulation of the gene. This regulatory region includes binding sites for critical transcription factors in the *IL2* promoter/enhancer region [18, 40, 41]. It has also been shown that the CpG site 1–specific methylation abrogates Oct-1/NFAT binding to the regulatory region and causes inhibition of *IL2* expression in Jurkat cells [18]. In the present study, we observed higher methylation in not only site 1 but all CpG sites in HIV-1 noncontrollers, suggesting that other CpG sites may be involved in *IL2* gene regulation by altering accessibility of chromatin and/or transcription factor binding.

IL-2 expression strongly depends on costimulatory signals through the CD28 superfamily of receptors during antigenic stimulation [40, 42]. It has been reported that the increase in histone acetylation and DNA demethylation at the *IL2* locus after T-cell receptor activation is impaired in the absence of CD28 costimulation [29, 30]. In this study, we observed increased levels of methylation of the *IL2* promoter only in terminally differentiated $CD4^+$ T cells without CD28 expression in HIV-1-uninfected individuals, supporting the idea that CD28 signaling plays an important role in DNA demethylation and/or remethylation of the *IL2* gene. However, we also observed DNA hypermethylation in early effector memory subsets with CD28 expression in HIV-1 noncontrollers, in which CD57 expression was abnormally elevated. In our experiments using HIV-1-uninfected subjects, CpG site 1 methylation was approximately 3-fold higher in $CD57^+$ versus $CD57^-$ memory $CD4^+$ T cells. Furthermore, we observed a positive correlation between CD57 expression in memory $CD4^+$ T cells and DNA methylation at CpG site 1 in the *IL2* promoter and also found a negative correlation between CD57 expression and IL-2 production in stimulated PBMCs. Taken together, our data indicate that CD57 engagement results in epigenetic modification of the *IL2* gene in a CD28-independent manner. The mechanism for gene regulation of CD28 and CD57 during the development of senescent T cells in the aged population remains unknown. Therefore, future studies should investigate molecular mechanisms underlying the relationship between the expression of IL-2 and these surface molecules. Of note, we observed no difference in *IL2* promoter DNA methylation in $CD8^+$ T cells. Meanwhile, it has been reported that IL-2 secretion in HIV-1-specific $CD8^+$ T cells was also impaired in progressors [7, 43]. Therefore, it is likely that mechanisms aside from DNA methylation regulate IL-2 expression. It will also be important for future studies to include analysis of epigenetic programs of effector molecules in HIV-1-specific T cells before and after cART initiation.

In the present study, we have identified epigenetic modification of the *IL2* promoter as a potential mechanism for the loss of IL-2 expression in $CD4^+$ T cells. This reprogramming of the *IL2* promoter may be coupled to the signaling events that also induce T-cell senescence during chronic HIV-1 infection. Individuals with chronic HIV-1 infection with a high viral load who maintained a certain $CD4^+$ T-cell count were recruited as noncontrollers, and individuals in late phase of HIV-1 infection and patients with AIDS were excluded in this study. Although there was no significant difference in $CD4^+$ T-cell count between controllers and noncontrollers in our cohort (by design), we observed DNA hypermethylation of the *IL2* locus in noncontrollers. In contrast, acutely infected individuals with a high viral load did not show the defect. These data suggest that $CD4^+$ T cells become senescent with loss of IL-2 expression before the decline in $CD4^+$ T-cell quantity if the immune system is persistently exposed persistently to high viral loads during chronic HIV-1 infection. Our data support the concept that early initiation of cART is a promising way to slow HIV-1 disease progression and immunosenescence.

Supplementary Data

Supplementary materials are available at *The Journal of Infectious Diseases* online (http://jid.oxfordjournals.org). Supplementary materials consist of data provided by the author that are published to benefit the reader. The posted materials are not copyedited. The contents of all supplementary data are the sole responsibility of the authors. Questions or messages regarding errors should be addressed to the author.

Notes

Acknowledgments. We thank all of the participants and clinical staff at the Research Hospital of the Institute of Medical Science, University of Tokyo, for their contributions.

Financial support. This work was supported by JSPS KAKENHI (grant 25293226 to A. K.-T.); the Ministry of Health, Labor, and Welfare of Japan (grants H24-AIDS-IPPAN-008 and H25-AIDS-IPPAN-007 to A. K.-T. and Research on International Cooperation in Medical Science, Research on Global Health Issues, and Health and Labor Science Research Grants H25-KOKUI-SITEI-001 to A. I.); Banyu Life Science Foundation International (grant to A. K.-T.); the Ministry of Education, Culture, Sports, Science and Technology (MEXT; contract 10005010 to A. I. and T. I., for the Program of Japan Initiative for Global Research Network on Infectious Diseases); and Global Centers of Excellence Program, MEXT (grant F06 to A. I.).

Potential conflicts of interest. A. K.-T. has received speaker's honoraria from ViiV Healthcare. A. I. has received grant support from Toyama Chemical, Astellas, ViiV Healthcare, MSD, and Baxter, through the University of Tokyo; and speaker's honoraria and payment for manuscript writing from Eiken Chemical, Astellas, Toyama Chemical, Torii Pharmaceutical, MSD, and Taisho Toyama Pharmaceutical. T. K. has received speaker's honoraria from Torii Pharmaceutical, MSD, ViiV Healthcare, Janssen Pharmaceutical, and AbbVie Inc. All other authors report no potential conflicts.

All authors have submitted the ICMJE Form for Disclosure of Potential Conflicts of Interest. Conflicts that the editors consider relevant to the content of the manuscript have been disclosed.

References

1. Appay V, Dunbar PR, Callan M, et al. Memory CD8+ T cells vary in differentiation phenotype in different persistent virus infections. Nat Med **2002**; 8:379–85.
2. Day CL, Kaufmann DE, Kiepiela P, et al. PD-1 expression on HIV-specific T cells is associated with T-cell exhaustion and disease progression. Nature **2006**; 443:350–4.
3. Kaufmann DE, Kavanagh DG, Pereyra F, et al. Upregulation of CTLA-4 by HIV-specific CD4+ T cells correlates with disease progression and defines a reversible immune dysfunction. Nat Immunol **2007**; 8: 1246–54.
4. Brenchley JM, Karandikar NJ, Betts MR, et al. Expression of CD57 defines replicative senescence and antigen-induced apoptotic death of CD8+ T cells. Blood **2003**; 101:2711–20.
5. Breton G, Chomont N, Takata H, et al. Programmed death-1 is a marker for abnormal distribution of naive/memory T cell subsets in HIV-1 infection. J Immunol **2013**; 191:2194–204.
6. Nakayama K, Nakamura H, Koga M, et al. Imbalanced production of cytokines by T cells associates with the activation/exhaustion status of memory T cells in chronic HIV type 1 infection. AIDS Res Hum Retroviruses **2012**; 28:702–14.
7. Betts MR, Nason MC, West SM, et al. HIV nonprogressors preferentially maintain highly functional HIV-specific CD8+ T cells. Blood **2006**; 107:4781–9.
8. Palmer BE, Boritz E, Wilson CC. Effects of sustained HIV-1 plasma viremia on HIV-1 Gag-specific CD4+ T cell maturation and function. J Immunol **2004**; 172:3337–47.
9. Ferrando-Martinez S, Casazza JP, Leal M, et al. Differential Gag-specific polyfunctional T cell maturation patterns in HIV-1 elite controllers. J Virol **2012**; 86:3667–74.
10. Potter SJ, Lacabaratz C, Lambotte O, et al. Preserved central memory and activated effector memory CD4+ T-cell subsets in human immunodeficiency virus controllers: an ANRS EP36 study. J Virol **2007**; 81:13904–15.
11. Wilson CB, Rowell E, Sekimata M. Epigenetic control of T-helper-cell differentiation. Nat Rev Immunol **2009**; 9:91–105.
12. Deaton AM, Webb S, Kerr AR, et al. Cell type-specific DNA methylation at intragenic CpG islands in the immune system. Genome Res **2011**; 21:1074–86.
13. Allan RS, Zueva E, Cammas F, et al. An epigenetic silencing pathway controlling T helper 2 cell lineage commitment. Nature **2012**; 487:249–53.
14. Lee GR, Kim ST, Spilianakis CG, Fields PE, Flavell RA. T helper cell differentiation: regulation by cis elements and epigenetics. Immunity **2006**; 24:369–79.
15. Youngblood B, Oestreich KJ, Ha SJ, et al. Chronic virus infection enforces demethylation of the locus that encodes PD-1 in antigen-specific CD8(+) T cells. Immunity **2011**; 35:400–12.
16. Youngblood B, Noto A, Porichis F, et al. Cutting edge: Prolonged exposure to HIV reinforces a poised epigenetic program for PD-1 expression in virus-specific CD8T cells. J Immunol **2013**; 191:540–4.
17. Bruniquel D, Schwartz RH. Selective, stable demethylation of the interleukin-2 gene enhances transcription by an active process. Nat Immunol **2003**; 4:235–40.
18. Murayama A, Sakura K, Nakama M, et al. A specific CpG site demethylation in the human interleukin 2 gene promoter is an epigenetic memory. EMBO J **2006**; 25:1081–92.
19. Kersh EN, Fitzpatrick DR, Murali-Krishna K, et al. Rapid demethylation of the IFN-gamma gene occurs in memory but not naive CD8T cells. J Immunol **2006**; 176:4083–93.
20. Ledderose C, Heyn J, Limbeck E, Kreth S. Selection of reliable reference genes for quantitative real-time PCR in human T cells and neutrophils. BMC Res Notes **2011**; 4:427.
21. Ishida T, Hamano A, Koiwa T, Watanabe T. 5' long terminal repeat (LTR)-selective methylation of latently infected HIV-1 provirus that is demethylated by reactivation signals. Retrovirology **2006**; 3:69.
22. Storey JD, Tibshirani R. Statistical significance for genomewide studies. Proc Natl Acad Sci U S A **2003**; 100:9440–5.
23. Holliday R, Pugh JE. DNA modification mechanisms and gene activity during development. Science **1975**; 187:226–32.
24. Jones PA, Liang G. Rethinking how DNA methylation patterns are maintained. Nat Rev Genet **2009**; 10:805–11.
25. Klose RJ, Bird AP. Genomic DNA methylation: the mark and its mediators. Trends Biochem Sci **2006**; 31:89–97.
26. Bird AP. CpG-rich islands and the function of DNA methylation. Nature **1986**; 321:209–13.
27. Gowers IR, Walters K, Kiss-Toth E, Read RC, Duff GW, Wilson AG. Age-related loss of CpG methylation in the tumour necrosis factor promoter. Cytokine **2011**; 56:792–7.
28. Lovinsky-Desir S, Ridder R, Torrone D, et al. DNA methylation of the allergy regulatory gene interferon gamma varies by age, sex, and tissue type in asthmatics. Clin Epigenetics **2014**; 6:9.
29. Thomas RM, Saouaf SJ, Wells AD. Superantigen-induced CD4+ T cell tolerance is associated with DNA methylation and histone hypo-acetylation at cytokine gene loci. Genes Immun **2007**; 8:613–8.
30. Thomas RM, Gao L, Wells AD. Signals from CD28 induce stable epigenetic modification of the IL-2 promoter. J Immunol **2005**; 174:4639–46.
31. Appay V, van Lier RA, Sallusto F, Roederer M. Phenotype and function of human T lymphocyte subsets: consensus and issues. Cytometry A **2008**; 73:975–83.
32. Romero P, Zippelius A, Kurth I, et al. Four functionally distinct populations of human effector-memory CD8+ T lymphocytes. J Immunol **2007**; 178:4112–9.
33. De Rosa SC, Brenchley JM, Roederer M. Beyond six colors: a new era in flow cytometry. Nat Med **2003**; 9:112–7.
34. Focosi D, Bestagno M, Burrone O, Petrini M. CD57+ T lymphocytes and functional immune deficiency. J Leukoc Biol **2010**; 87:107–16.
35. Palmer BE, Blyveis N, Fontenot AP, Wilson CC. Functional and phenotypic characterization of CD57+CD4+ T cells and their association with HIV-1-induced T cell dysfunction. J Immunol **2005**; 175:8415–23.
36. Kern F, Ode-Hakim S, Vogt K, Hoflich C, Reinke P, Volk HD. The enigma of CD57+CD28- T cell expansion–anergy or activation? Clin Exp Immunol **1996**; 104:180–4.
37. Monteiro J, Batliwalla F, Ostrer H, Gregersen PK. Shortened telomeres in clonally expanded CD28-CD8+ T cells imply a replicative history that is distinct from their CD28+CD8+ counterparts. J Immunol **1996**; 156:3587–90.
38. Strioga M, Pasukoniene V, Characiejus D. CD8+ CD28- and CD8+ CD57+ T cells and their role in health and disease. Immunology **2011**; 134:17–32.
39. Harari A, Vallelian F, Pantaleo G. Phenotypic heterogeneity of antigen-specific CD4T cells under different conditions of antigen persistence and antigen load. Eur J Immunol **2004**; 34:3525–33.

40. Schwartz RH. Costimulation of T lymphocytes: the role of CD28, CTLA-4, and B7/BB1 in interleukin-2 production and immunotherapy. Cell **1992**; 71:1065–8.
41. Garrity PA, Chen D, Rothenberg EV, Wold BJ. Interleukin-2 transcription is regulated in vivo at the level of coordinated binding of both constitutive and regulated factors. Mol Cell Biol **1994**; 14: 2159–69.
42. Sanchez-Lockhart M, Marin E, Graf B, et al. Cutting edge: CD28-mediated transcriptional and posttranscriptional regulation of IL-2 expression are controlled through different signaling pathways. J Immunol **2004**; 173:7120–4.
43. Zanussi S, Simonelli C, D'Andrea M, et al. CD8+ lymphocyte phenotype and cytokine production in long-term non-progressor and in progressor patients with HIV-1 infection. Clin Exp Immunol **1996**; 105:220–4.

PLOS ONE

Development and Customization of a Color-Coded Microbeads-Based Assay for Drug Resistance in HIV-1 Reverse Transcriptase

Lijun Gu[1,2], Ai Kawana-Tachikawa[3], Teiichiro Shiino[4], Hitomi Nakamura[5,6], Michiko Koga[3,6], Tadashi Kikuchi[3,6], Eisuke Adachi[6], Tomohiko Koibuchi[6], Takaomi Ishida[1,2], George F. Gao[7], Masaki Matsushita[8], Wataru Sugiura[4], Aikichi Iwamoto[1,3,5,6], Noriaki Hosoya[3,5]*

1 Research Center for Asian Infectious Diseases, the Institute of Medical Science, the University of Tokyo, Tokyo, Japan, **2** Japan-China Joint Laboratory of Molecular Immunology and Molecular Microbiology, Institute of Microbiology, Chinese Academy of Sciences, Beijing, P. R. China, **3** Division of Infectious Diseases, Advanced Clinical Research Center, the Institute of Medical Science, the University of Tokyo, Tokyo, Japan, **4** AIDS Research Center, National Institute of Infectious Diseases, Tokyo, Japan, **5** Department of Infectious Disease Control, International Research Center for Infectious Diseases, the Institute of Medical Science, the University of Tokyo, Tokyo, Japan, **6** Division of Infectious Diseases and Applied Immunology, Research Hospital, The Institute of Medical Science, The University of Tokyo, Tokyo, Japan, **7** CAS Key Laboratory of Pathogenic Microbiology and Immunology, Institute of Microbiology, Chinese Academy of Sciences, Beijing, P. R. China, **8** Biotech Research and Development, Wakunaga Pharmaceutical Corporation, Hiroshima, Japan

Abstract

Background: Drug resistance (DR) of HIV-1 can be examined genotypically or phenotypically. Although sequencing is the gold standard of the genotypic resistance testing (GRT), high-throughput GRT targeted to the codons responsible for DR may be more appropriate for epidemiological studies and public health research.

Methods: We used a Japanese database to design and synthesize sequence-specific oligonucleotide probes (SSOP) for the detection of wild-type sequences and 6 DR mutations in the clade B HIV-1 reverse transcriptase region. We coupled SSOP to microbeads of the Luminex 100 xMAP system and developed a GRT based on the polymerase chain reaction (PCR)-SSOP-Luminex method.

Results: Sixteen oligoprobes for discriminating DR mutations from wild-type sequences at 6 loci were designed and synthesized, and their sensitivity and specificity were confirmed using isogenic plasmids. The PCR-SSOP-Luminex DR assay was then compared to direct sequencing using 74 plasma specimens from treatment-naïve patients or those on failing treatment. In the majority of specimens, the results of the PCR-SSOP-Luminex DR assay were concordant with sequencing results: 62/74 (83.8%) for M41, 43/74 (58.1%) for K65, 70/74 (94.6%) for K70, 55/73 (75.3%) for K103, 63/73 (86.3%) for M184 and 68/73 (93.2%) for T215. There were a number of specimens without any positive signals, especially for K65. The nucleotide position of A2723G, A2747G and C2750T were frequent polymorphisms for the wild-type amino acids K65, K66 and D67, respectively, and 14 specimens had the D67N mutation encoded by G2748A. We synthesized 14 additional oligoprobes for K65, and the sensitivity for K65 loci improved from 43/74 (58.1%) to 68/74 (91.9%).

Conclusions: We developed a rapid high-throughput assay for clade B HIV-1 DR mutations, which could be customized by synthesizing oligoprobes suitable for the circulating viruses. The assay could be a useful tool especially for public health research in both resource-rich and resource-limited settings.

Citation: Gu L, Kawana-Tachikawa A, Shiino T, Nakamura H, Koga M, et al. (2014) Development and Customization of a Color-Coded Microbeads-Based Assay for Drug Resistance in HIV-1 Reverse Transcriptase. PLoS ONE 9(10): e109823. doi:10.1371/journal.pone.0109823

Editor: Nicolas Sluis-Cremer, University of Pittsburgh, United States of America

Received May 7, 2014; **Accepted** September 10, 2014; **Published** October 14, 2014

Data Availability: The authors confirm that all data underlying the findings are fully available without restriction. All relevant data are within the paper.

Funding: This work was supported in part by a contract research fund from the Ministry of Education, Culture, Sports, Science and Technology (MEXT) for Program of Japan Initiative for Global Research Network on Infectious Diseases (10005010)(AI); Global COE Program (Center of Education and Research for Advanced Genome-Based Medicine - For personalized medicine and the control of worldwide infectious diseases -) of MEXT (F06)(AI); JSPS KAKENHI (25293226)(AKT); JSPS KAKENHI (24790437, 26860300)(NH);Grants for AIDS research from the Ministry of Health, Labor, and Welfare of Japan (H24-AIDS-IPPAN-008)(AKT); Grants for AIDS research from the Ministry of Health, Labor, and Welfare of Japan (H25-AIDS-IPPAN-006)(NH); Research on international cooperation in medical science, Research on global health issues, Health and Labour Science Research Grants, the Ministry of Health, Labor, and Welfare of Japan (H25-KOKUI-SITEI-001)(AI). The funders had no role in study design, data collection and analysis, decision to publish, or preparation of the manuscript.

Competing Interests: A.I. has received grant support from Toyama Chemical Co. Ltd., astellas, ViiV Healthcare K.K., MSD K.K., Baxter through the University of Tokyo. A.I. has received speaker's honoraria/payment for manuscript from Eiken Chemical Co. Ltd., astellas, Toyama Chemical Co. Ltd, Torii Pharmaceutical Co. Ltd., Takeda Pharmaceutical Co. Ltd. and MSD. MM is an employee of Wakunaga Pharmaceutical Corporation which keeps a patent on PCR amplification sequence-specific oligonucleotide probes (SSOP) method. For the remaining authors none were declared. This does not alter the authors' adherence to PLOS ONE policies on sharing data and materials.

* Email: hnori@ims.u-tokyo.ac.jp

Introduction

Since combination antiretroviral therapy (cART) was introduced, the prognosis of patients with HIV-1 infection has improved dramatically [1,2]. In resource-rich settings, new classes, new drugs or new formulations of previously-known classes of antiretroviral drugs (ARV) have been introduced continuously for clinical use. Nucleoside/nucleotide reverse transcriptase inhibitor (NRTI) resistance has declined over time in resource-rich settings, presumably reflecting the improvement of treatment regimens [3,4]. Rates of transmitted HIV-1 drug resistance (DR) have remained limited also in resource-limited settings; however, limitation of the first-line and subsequent regimens would be a concern. cART consisting of two NRTIs and one non-nucleoside reverse transcriptase inhibitors (NNRTI), most often zidovudine (AZT) + lamivudine (3TC) or stavudine (d4T) + 3TC plus nevirapine (NVP) or efavirenz (EFV), has been widely used as the treatment regimen in the resource-limited settings [5,6]; consequently, DR might become a larger public health challenge in the developing countries.

DR can be examined genotypically or phenotypically [7] (http://www.aidsmap.com/pdf/Resistance-tests/page/1044559/). Although sequencing is the gold standard of the genotypic resistance testing (GRT), high-throughput GRT targeted to the codons responsible for DR may be more convenient and suitable for public health research [8,9]. We applied the PCR-SSOP-Luminex method [10–12] to an HIV-1 GRT. As an initial approach, we focused on designing an assay for six major DR mutations: M41L, K65R, K70R, K103N, M184V and T215Y/F. M41L, K70R, T215F/Y are examples of thymidine analogue mutations (TAMs) and associated with AZT and d4T [13] (HIV Drug resistance database, Stanford University, http://hivdb.stanford.edu/index.html). K65R is associated multi-nucleoside and nucleotide DR. Although K65R is selected by nucleotide reverse transcriptase inhibitor tenofovir (TDF) usually, it can be selected by d4T. K103N is highly associated with EFV and NVP resistance. The K103N mutation reduces susceptibility to NVP by 50-flod, and EFV by 20-fold. M184V is highly associated with 3TC and emtricitabine (FTC) resistance, and reduce the susceptibility to 3TC by 200-fold. The monitoring of these six DR mutations should be important for molecular epidemiologic study estimating the efficacy of anti-HIV drugs especially in resource limited settings. We synthesized the oligonucleotides for the primers and probes based on the Japanese data base on reverse transcriptase mutations. In order to validate the initial assay system and examine the flexibility for customization, we focused on the clade B HIV-1 which is most prevalent in Japan. Here we report the results of the comparison between sequencing and the PCR-SSOP-Luminex assay using the specimens of a Japanese cohort.

Methods

PCR-SSOP-Luminex assay

HIV-1 DR genotyping described here is based on the reverse SSOP method coupled with a microsphere beads array platform (Luminex Corporation, Austin, TX, USA). Briefly, the method involves PCR amplification by biotinylated primers, hybridization to nucleotide probes coupled to microbeads, detection of the bound PCR products by streptavidin-phycoerythrin (SAPE) reaction, and quantitation by measurement of median fluorescence intensity (MFI).

Color-coded microbeads were coupled to oligoprobes derived from DR mutations or conserved sequences in HIV-1 RT coding region. These synthesized probes were modified at the 5′-end with a terminal amino group and covalently bound to the carboxylated fluorescent microbeads using ethylene dichloride (EDC), following the procedures recommended by the manufacturer (Wakunaga Pharmaceutical Co. Ltd, Hiroshima, Japan). Briefly, 6.25×10^5 carboxylated microbeads were suspended in 50 µl of 0.1 M MES (2-(N-morpholino) ethane sulfonic acid, pH 4.5 (Dojindo Laboratories, Kumamoto Techno Research Park, Kumamoto, Japan). Afterwards, 0.5 µM of amine-substituted oligonucleotide probes was added, followed by 100 mg/ml EDC (1-Ethyl-3-(3-dimethylaminopropyl) carbodiimido hydrochloride) (Pierce Biotechnology, Rockford, IL, USA), and the mixture was incubated in the dark for 30 min at 25°C. The EDC addition and incubation were repeated twice and the microbeads were washed once with 0.02% Tween-20 and once with 0.1% SDS. After the final wash, the pellets were resuspended in 50 µl TE buffer (pH 8.0), and counted on a hemocytometer. The concentration of fluorescence-labeled microbeads coupled to oligonucleotide probes (oligobeads) was adjusted to 8000–12000/µl, and oligobeads were stored at 4°C in the dark.

Five-microliter aliquots of the 5′-biotinlabeled amplified DNA were added to wells in a 96-well PCR tray containing 5 µl/well of denaturation solution, and allowed to denature for 5 min at RT. Hybridization mixture was prepared using oligobeads stocks, SAPE and hybridization solution, according to the manufacturer's instructions (Wakunaga Pharmaceutical Co. Ltd, Hiroshima, Japan). Twenty-five-microliter aliquots of hybridization mixture containing 500 each sequence-specific oligobeads were added to each well. The amplicons were hybridized at 55°C for 30 min using the thermal cycler. Hybridized amplicons were washed twice with 75 µl of wash solution in each well. Reaction outcomes were measured by the Luminex 100 flow cytometer that is equipped with two types of lasers. The bead populations were detected and identified using the 635 nm laser. The SAPE fluorescence of the biotin labeled amplicons that had hybridized to the oligobeads was quantitated using the 532 nm laser. The MFI of SAPE was used to quantify the amount of DNA bound to the oligobeads. Assays were performed in triplicate.

Site-directed mutagenesis and plasmid construction

To assess the feasibility of the assay system, we chose cloned SF2 genome (GenBank accession number K02007) as a template. Synthesized PCR fragments with DR mutations created by site-directed mutagenesis were inserted into the SF2 genome. The numbering system used to refer to DR mutations was based on HXB2 genome (HXB2 location 2485–3309, GenBank accession number K03455) sequences. The SF2 and HXB2 genome had the same sequence in the regions covered by the probes.

Plasmid p9B/R7 from the HIV-1 SF2 strain was a kind gift of Dr. T. Shioda (Osaka University, Osaka, Japan) [14,15]. An *Xho* I- *BamH* I fragment including the pol gene from p9B/R7 was subcloned into pBluescript II SK (+) (Stratagene, La Jolla, CA, USA). As shown in Fig. 1A, various DR mutations were introduced into the *Xho* I- *BamH* I fragment of the plasmid by site-directed mutagenesis using oligonucleotides and PCR methods as previously described [16], and were confirmed by sequencing.

Clinical specimens

Sixty subjects were selected from among patients participating in an ongoing study on microbes at an HIV outpatient clinic affiliated with the Institute of Medical Science, the University of Tokyo (IMSUT). The study was approved by the internal review board of IMSUT (20-31-1120), and all subjects provided written informed consent. The median HIV-1 RNA and CD4 cells count

A

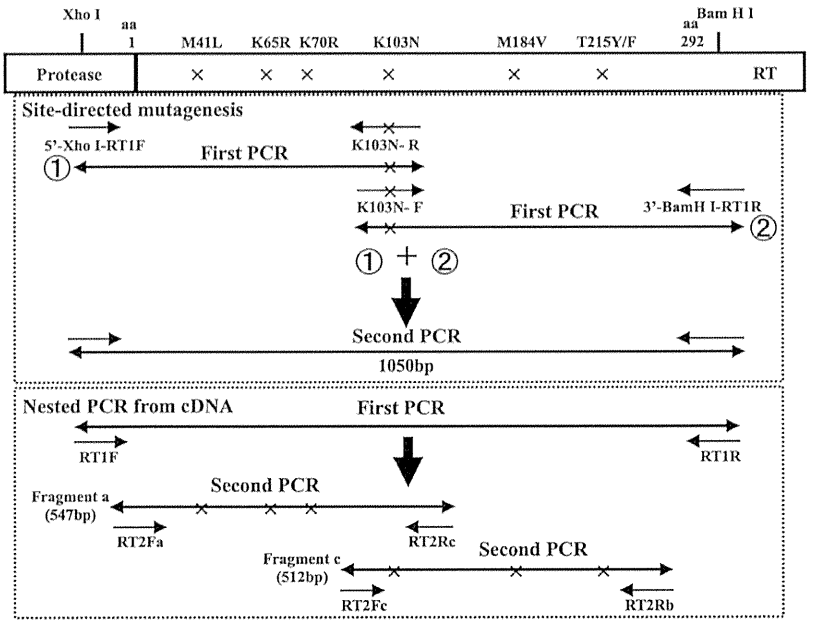

B

PCR primers

RT1F: 5'-ATGATAGGGGGAATTGGAGGTTT- 3'

RT1R: 5'- TACTTCTGTTAGTGCTTTGGTTCC- 3'

RT2Fa: 5'- GACCTACACCTGTCAACATAATTGG- 3'

RT2Rc: 5'- TGGAATATTGCTGGTGATCC- 3'

RT2Fc: 5'-AACTCAAGACTTCTGGGAAGT- 3'

RT2Rb: 5'-CAGTCCAGCTGTCTTTTTCTGGC- 3'

Sequencing primers

T7: 5′-TAATACGACTCACTATAGGG-3′

Rev: 5′-CAGGAAACAGCTATGAC-3′

Figure 1. Schematic representation of PCR amplification and sequences of primers for PCR and sequencing. (A) Top: Site-directed mutagenesis using oligonucleotide is shown using K103N as an example. Desired mutations in the reverse transcriptase gene were engineered in two PCR fragments, then incorporated into a larger fragment (1050 bp, HXB2 location 2388–3425) by the second PCR, and cloned into pBluescript II SK (+) at *XhoI*-*BamHI* sites. Bottom: Negative strand cDNA was synthesized from patients' plasma. After the first strand PCR using RT1F and RT1R as primers, Fragment a or Fragment c were amplified by nested PCR. (B) Primer sequences for PCR amplification and sequencing.
doi:10.1371/journal.pone.0109823.g001

at sampling were 4.15 (range 2.60–5.88) log 10 copies/ml and 264 (range: 9–902) cells/μl, respectively. Seventy-four specimens from 60 patients were analyzed in this study. Forty-eight patients contributed one plasma specimen, 10 patients contributed two plasma specimens from different time points, and two patients contributed three separate plasma specimens. Twenty-two specimens were from patients who were treatment-naïve when the plasma specimens were obtained. The remaining 52 specimens were from patients on failing treatment including NRTI at the time of sample collection.

Viral RNA extraction, cDNA synthesis, and PCR amplification

Viral RNA was extracted from 140 μl plasma using QIAamp Viral RNA Mini Kit (QIAGEN, Valencia, CA, USA) and eluted

Table 1. Design of oligoprobes based on clade B HIV-1 sequences from Japanese surveillance database.

Locus	genetic code	Frequency(%)	Name of probe	Oligoprobes	Nucleotide sequence (5'-3')	100% match isolates of database
M41					TGT ACA GAA ATG GAA	
	M41-ATG	795/795(100)	M41M-ATG	GTACAGAAATGGAA	— --- --- --- ---	618/868(71.2%)
	M41L-TTG	109/180(60.6)	M41L-TTG	GTACAGAATTGGAA	— --- --- T— ---	
	M41L-CTG	69/180(38.3)	M41L-CTG	GTACAGAACTGGAA	— --- --- C— ---	
	M41L-TTA	1/180(0.6)				
	M41L-TTR	1/180(0.6)				
K65					ATA AAG AAA AAA GAC AGT	
	K65-AAA	961/1012(95.0)	K65K-AAA	ATAAAGAAAAAAGACAG	--- --- --- --- --- —	516/870(59.3%)
	K65-AAG	30/1012(3.0)				
	K65-AAR	21/1012(2.1)				
	K65R-AGA	7/7(100)	K65R-AGA	ATAAAGAGAAAAGACAG	--- --- -G- --- --- —	
	K65R-AGG	0/7(0.0)				
K70					GAC AGT ACT AAA TGG AGA	
	K70-AAA	849/885(95.9)	K70K-AAA-1	GACAGTACTAAATG	--- --- --- --- —	621/769(80.8%)
			K70K-AAA-2	GTACTAAATGGAGA	--- --- --- --- ---	
	K70-AAG	17/885(1.9)				
	K70-AAR	19/885(2.1)				
	K70R-AGA	85/88(96.6)	K70R-AGA	GTACTAGATGGAGA	--- --- -G- --- ---	
	K70R-AGG	0/88(0.0)	K70R-AGG	GTACTAGGTGGAGA	--- --- -GG --- ---	
	K70R-AGR	3/88(3.4)				
K103					TTA AAA AAG AAA AAA TCA GTA	
	K103-AAA	815/867(94.0)	K103K-AAA	AAAAAAGAAAAAATCAG	- --- --- --- --- --- -	558/785(71.1%)
	K103-AAG	25/867(2.9)				
	K103-AAR	27/867(3.1)				
	K103N-AAC	112/128(87.5)	K103N-AAC	AAAAAAGAACAAATCAG	- --- --- —C --- --- -	
	K103N-AAT	3/128(2.3)	K103N-AAT	AAAAAAGAATAAATCAGT	- --- --- —T --- --- —	
	K103N-AAY	13/128(10.2)				
M184					TAT CAA TAC ATG GAT GAT	
	M184-ATG	659/659(100)	M184M-ATG	TATCAATACATGGATG	--- --- --- --- --- -	761/888(85.7%)
	M184V-GTG	295/335(88.1)	M184V-GTG	TATCAATACGTGGATG	--- --- --- G— --- -	
	M184V-GTA	14/335(4.2)				
	M184V-GTR	26/335(7.8)				
T215					TGG GGA TTT ACC ACA CCA	
	T215-ACC	692/724(95.6)	T215T-ACC-1	GGGGATTTACCACA	— --- --- --- ---	583/813(71.7%)
			T215T-ACC-2	GGGGATTTACCACACCA	— --- --- --- --- ---	
	T215-ACT	13/724(1.8)				
	T215-ACA	7/724(1.0)				
	T215-ACG	3/724(0.4)				
	T215-ACY	8/724(1.1)				
	T215-ACM	1/724(0.1)				
	T215F-TTC	54/54(100)	T215F-TTC	GGGGATTTTTCACAC	— --- --- TT- ---	
	T215Y-TAC	182/185(98.4)	T215Y-TAC	GGGGATTTTACACAC	— --- --- TA- --- -	
	T215Y-TAT	2/185(1.1)				
	T215Y-TAY	1/185(0.5)				
Standard probes			S2582	ATTAAAGCCAGGAATGGAT		
			S2693	AAAAATTGGGCCTGAAAAT		
			S3230	CCTTTGGATGGGTTATGAA		
			S3252	CATCCTGATAAATGGACAG		

Table 1. Cont.

Locus	genetic code	Frequency(%)	Name of probe	Oligoprobes	Nucleotide sequence (5'-3')	100% match isolates of database
			53243	TATGAACTCCATCCTGA		

R: Mixed base of A and G; Y: Mixed base of C and T; M: Mixed base of C and A.
doi:10.1371/journal.pone.0109823.t001

with 60 μl AVE buffer. For cDNA synthesis, 55 μl of RNA solution was mixed with 5 μl of 100 pmol/μl random primer (TaKaRa Bio, Otsu, Shiga, Japan) or specific primer, RT1R (Fig. 1B), and 5 μl of 10 mM dNTPs, and denatured at 70°C for 10 min. The RT mixture containing 20 μl of 5× First-Strand buffer, 5 μl of 0.1 M DTT, 5 μl of RNaseOUT Recombinant RNase inhibitor (40 U/μl; Invitrogen, Carlsbad, California, USA) and 5 μl of SuperScript III RT (200 U/μl, Invitrogen) was added to the 65 μl denatured viral RNA-primer-dNTP mixture. The reaction mixture (100 μl final volume) was incubated at 25°C for 5 min for annealing and then at 55°C for 60 min for reverse transcription. The reaction was inactivated by heating at 70°C for 15 min.

RT gene fragments were amplified by nested PCR from cDNAs or by single PCR from plasmids. For the first reaction a 1050 bp fragment from the RT coding region was amplified from 5 μl aliquots of cDNAs using RT1F and RT1R as outer primers in a reaction mixture containing 50 μl of 1×Prime STAR buffer, 0.2 mM of each dNTPs, 0.5 μM of each primer, and 0.5 μl Prime STAR HS DNA Polymerase (25 U/μl, TaKaRa Bio, Otsu, Shiga, Japan). Amplification conditions consisted of 35 cycles denaturation at 98°C for 10 s, annealing at 55°C for 5 s, and extension at 72°C for 30 s.

For the second reaction of the nested PCR and for the single PCR from plasmids (0.1 pg), RT coding fragments were amplified in two PCR fragments using two 5′ biotinylated primer sets, PS1 and PS2, as described previously [17]. The PS1 primer set produced a 547 bp amplicon that was used to detect M41L, K65R, K70R, and K103N, and the PS2 primer set produced a 512 bp amplicon that was used to detect K103N, M184V, and T215Y/F (Fig. 1A). The reaction mixture used 5 μl of the first PCR products or 0.1 pg of plasmid DNA in a final volume of 50 μl, as described above, with amplification conditions as follows: 25 cycles (second nested PCR) or 35 cycles (plasmid DNA amplification) of denaturation at 98°C for 10 s, annealing at 55°C for 5 s, and extension at 72°C for 1 min. The PCR amplicons were used for Luminex detection or direct sequencing.

Sequencing

PCR products were purified with the QIAquick PCR Purification Kit (QIAGEN, Valencia, CA, USA) and were directly sequenced in both directions using ABI 3130xl genetic analyzer (Applied Biosystems, Foster City, CA, USA) and Big Dye terminator V3.1 cycle sequencing kit (Applied Biosystems). In the case of sequence ambiguity due to a coexistence of multiple nucleotides, we confirmed the sequence by cloning and sequencing. For cloning and sequencing, the purified PCR fragments were phosphorylated using T4 polynucleotide kinase (TaKaRa Bio, Otsu, Shiga, Japan) and inserted into the dephosphorylated *EcoR*V restriction site of pBluescript II SK(+). Inserts were sequenced using T7 and Rev universal primers (Fig. 1B).

HIV-1 Japanese surveillance database

In Japan 10 university hospitals, 5 medical centers, 5 public health laboratories, and the National Institute of Infectious Diseases are collaborating in the surveillance of newly diagnosed HIV/AIDS cases. HIV/AIDS patients with both acute and chronic infections, newly diagnosed at these centers since January 2003 were enrolled [18]. Prevalence of DR codons in these patients was determined by analysis of sequences of clade B HIV-1 reverse transcriptase positions 1–240 amino acids.

Statistical analysis

GraphPad Prism 5.0 software (GraphPad Software Inc., San Diego, CA) was used for statistical data analysis. Statistical significance was defined as $P<0.05$.

Results

Design of oligoprobes based on the database of clade B HIV-1 sequences in Japan

Based on the frequency of the codon usage in the Japanese surveillance database for amino acids M41, K65, K70, K103, M184 and T215 in RT gene, we designed the nucleotide sequence of 18 oligoprobes for DR mutation and 5 standard probes (Table 1). We adopted nucleotide sequences of HXB2 strain for the flanking sequences. Synthesized oligoprobes could cover 71.2%, 59.3%, 80.8%, 71.1%, 85.7% and 71.7% of M41, K65, K70, K103, M184 and T215, respectively (Table 1). Five standard probes were designed in the conserved region of RT gene and used as the assay control.

Evaluation of PCR-SSOP-Luminex DR assay using cloned HIV-1

We examined the sensitivity and specificity of the PCR-SSOP-Luminex DR assay using cloned HIV-1. The test fragments were amplified (Fig. 2A), and the amplicons were hybridized to the 16 oligobeads. We performed three independent assays with triplicate hybridization and detection in each assay. The mean positive signal and standard deviation were 5237±1398 (Fig. 2B). The CV% of positive signal and standard deviation were 10.1% ±10.7. The mean of negative signal and standard deviation were 131.2±69.4. The CV% of negative signal and standard deviation were 21.6±23.6 (mean ± S.D.). MFIs of hybridization signals were clearly high only when the oligoprobes matched the mutations in the fragments (Fig. 2B). These data confirmed that the assay system could discriminate one base mismatch at M41, K65, K70, K103, M184 and T215 codons in the plasmid-probe model system.

Next, we examined the sensitivity to detect a particular sequence in a mixture for each DR-related site. The plasmids carrying the wild type and mutant sequences were mixed at various ratios. In samples containing only the wild type sequences, the mean background signal (% ±2SD) was 2.0% ±1.2, 4.1%

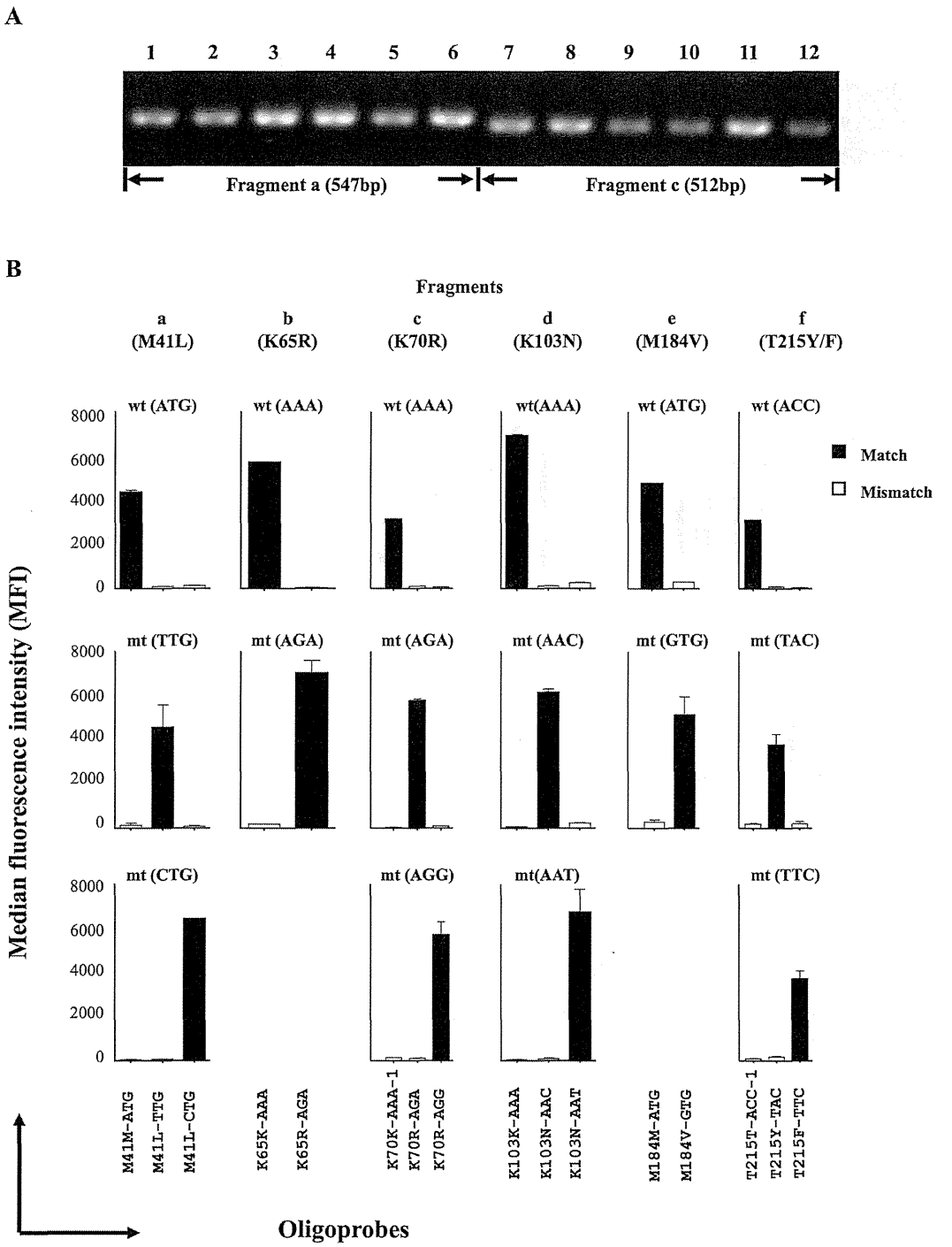

Figure 2. Validation of PCR-SSOP-Luminex assay using plasmids as templates. (A) Agarose gel electrophoresis of amplified fragments. Lanes 1–6: Fragment a (547 bp). Lanes 7–14: Fragment c (512 bp). 1, wild type; 2, M41L-TTG; 3, M41L-CTG; 4, K65R-AGA; 5, 70R-AGA; 6, 70R-AGG; 7, wild type; 8, 103N-AAC; 9, K103N-AAT; 10, M184V-GTG; 11, T215Y-TAC; 12, T215F-TTC. (B) Median fluorescence intensities (MFIs). The plasmid in the test sample is indicated on the top of each panel. Oligoprobes used for detection are indicated at the bottom. Matched results are shown as black bars, mismatched results as white bars. Assays were performed in triplicate. The mean ± standard deviation is shown at the top of each bar.
doi:10.1371/journal.pone.0109823.g002

±2.6, 3.3% ±1.2, 4.6% ±1.8, 6.2% ±3.2 and 3.3% ±0.4 at M41, K65, K70, K103, M184 and T215, respectively (Fig. 3B). The signal for the mutant was judged positive when "% signal" from the mutant oligobeads exceeded the mean + 2SD; 3.2%,

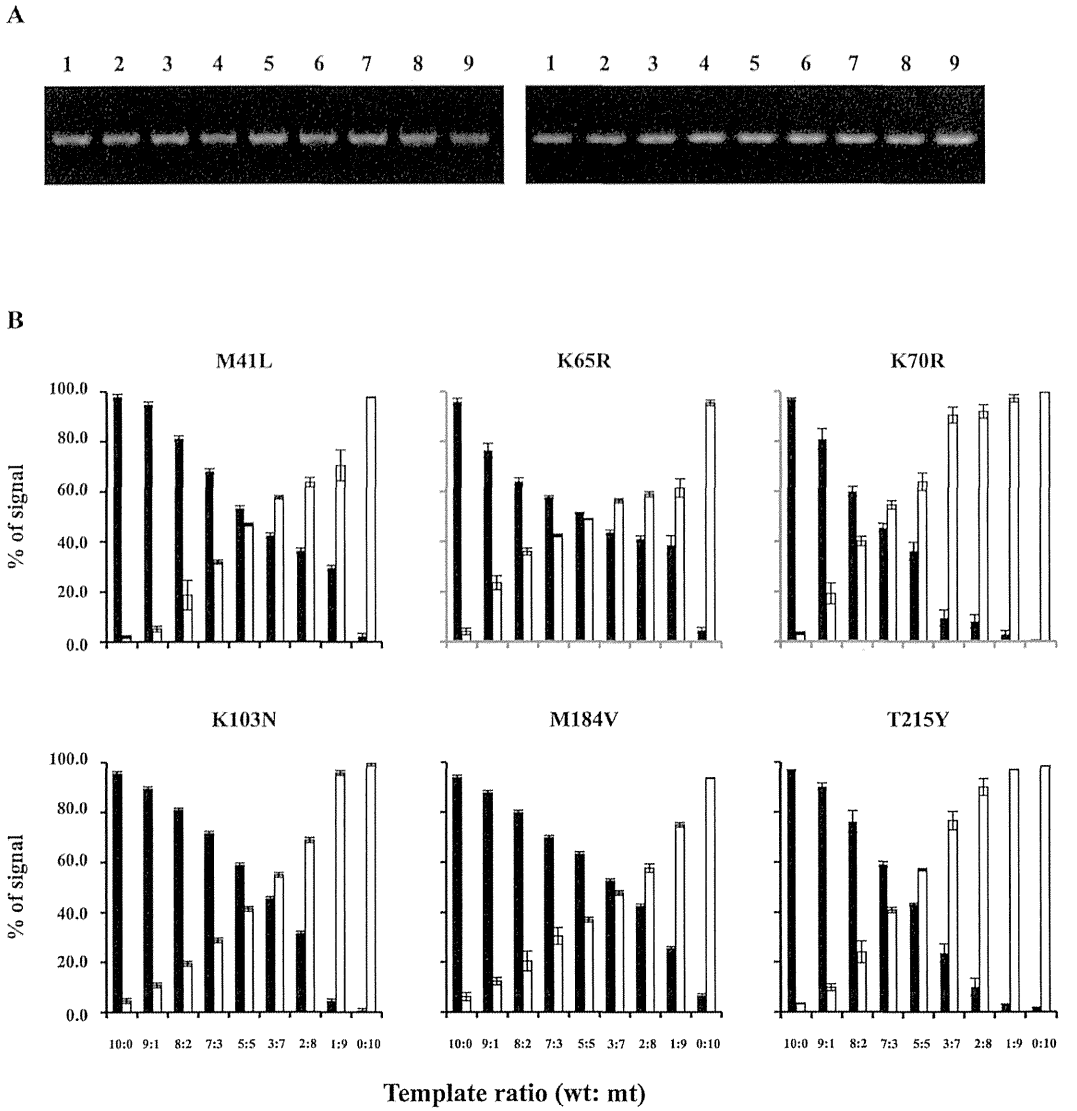

Figure 3. Assay sensitivity in a mixture. (A) Agarose gel electrophoresis of mixtures of amplified fragments. Left panel: Fragment a (547 bp). Right panel: Fragment c (512 bp). Wild-type:mutant ratio; Lanes 1 (10:0); 2 (9:1); 3 (8:2); 4 (7:3); 5 (5:5); 6 (3:7); 7 (2:8); 8 (1:9); 9 (0:10). (B) Signals from wild type probes (black bars) and mutant probes (white bars) in each mixture. "% of signal" was calculated by "MFI of wild type or mutant signal" divided by "MFI of wild type plus mutant signal" and multiplied by 100. Triplicate experiments were performed three times. "% of signal" is shown with standard deviations.
doi:10.1371/journal.pone.0109823.g003

6.7%, 4.5%, 6.4%, 9.4%, 3.7% at M41, K65, K70, K103, M184 and T215, respectively. Actual signals from the mutant oligoprobes at 9:1 (wild type:mutant) mixture at these sites was 5.1%, 23.6%, 19.2%, 10.7%, 12.3%, 9.8%, respectively. Therefore, we infer that the assay can detect 10% DR mutants in the population. There was a big variation (5.1 to 23.6%) in detection of 10% mixtures. We suppose that the difference in minor variant detection could be caused by the melting temperature (GC content and length). Although we compared the GC content and probe length, we could not find a reasonable explanation from this list (data not shown).

Identification of DR mutations in clinical specimens by sequencing

In order to determine the sequence, we amplified the RT gene in two separate fragments from frozen plasma (Fig. 1A). We succeeded to amplify fragment a (containing M41, K65, K70) from all 74 specimens, but failed to amplify fragment c (containing K103, M184, T215) in one patient. Infection with clade B HIV-1 was confirmed by phylogenetic analysis of the RT gene. DR mutations were found at codons M41L (n = 22), K65R (n = 3), K70R (n = 10), K103N (n = 7), M184V (n = 21) and T215Y/F (n = 22) in 40 specimens (Table 2).

Table 2. Comparison of the results between sequencing and PCR-SSOP-Luminex assay.

Position	Aminoacid	Codons	Number of specimens (percentage)	
			Direct sequencing	PCR-SSOP-Luminex
41	Met	ATG	52 (70.3)	41 (55.4)
	Leu	TTG	16 (21.6)	16 (21.6)
		CTG	5 (6.8)	5 (6.8)
	Met, Leu mix		1 (1.4)	0
	No reaction		-	12 (16.2)
65	Lys	AAA	64 (86.5)	41 (55.4)
		AAG	4 (5.4)	0
		AAA, AAG mix	3 (4.1)	2 (2.7)
	Arg	AGA	3 (4.1)	0
	No reaction		-	31 (41.9)
70	Lys	AAA	62 (83.8)	61 (82.4)
		AAG	2 (2.7)	0
	Arg	AGA	8 (10.8)	8 (10.8)
		AGG	1 (1.4)	1 (1.4)
	Lys, Arg mix		1 (1.4)	0
	No reaction		-	4 (5.4)
103	Lys	AAA	60 (82.2)	50 (68.5)
		AAG	1 (1.4)	0
		AAA, AAG mix	1 (1.4)	0
	Asn	AAC	4 (5.5)	2 (2.7)
		AAT	2 (2.7)	2 (2.7)
		AAC, AAT mix	1 (1.4)	1 (1.4)
	Arg	AGA	4 (5.5)	0
	No reaction		-	18 (24.7)
184	Met	ATG	52 (71.2)	46 (63.0)
	Val	GTG	19 (26.0)	16 (21.9)
		GTA	1 (1.4)	0
	Met, Val mix		1 (1.4)	1 (1.4)
	No reaction		-	10 (13.7)
215	Thr	ACC	48 (65.8)	46 (63.0)
	Tyr	TAC	16 (21.9)	15 (20.5)
	Phe	TTC	6 (8.2)	6 (8.2)
	Thr, Tyr mix		1 (1.4)	1 (1.4)
	Other		2 (2.7)	0
	No reaction		-	5 (6.8)

doi:10.1371/journal.pone.0109823.t002

Identification of DR mutations in clinical specimens by the PCR-SSOP-Luminex DR assay

We performed the PCR-SSOP-Luminex DR assay on 74 specimens whose DR mutations had been sequenced (Fig. 4). The lowest MFI of five standard probes (MFI = 837.5) was assumed as the cut off value for the positive signal. We synthesized two additional wild-type oligoprobes (K70K-AAA-2 and T215T-ACC-2), since the original oligobeads (K70K-AAA-1 and T215T-ACC-1) gave marginal signals in some specimens (Table 1 and Fig. 4). By the modification of the position of the target codons and the length of flanking sequences, we could obtain higher MFI signals. Successful determination of the genotypes was 62/74 (83.8%), 43/74 (58.1%), 70/74 (94.6%), 55/73 (75.3%), 63/73 (86.3%) and 68/73 (93.2%) for M41, K65, K70, K103, M184 and T215, respectively. The median of background signal (without sample) was MFI = 178, and median negative signal from the patients sample was MFI = 181 (interquartile range (IQR) = 101–307). PCR-SSOP-Luminex assays create very low background and non-specific signal from negative samples. When the genotype was successfully determined by the PCR-SSOP-Luminex assay, the results were always concordant with those of sequencing (Table 2). We inferred that the failure to determine the genotype was due to sequence diversities. Therefore, we decided to customize the assay according to the sequences around K65 which had the lowest success rate (58.1%).

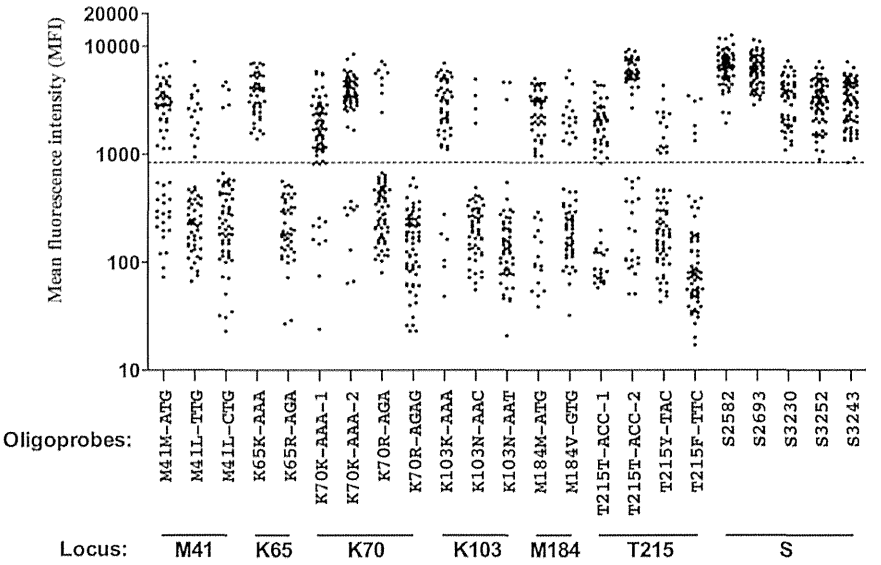

Figure 4. PCR-SSOP-Luminex DR assay of clinical samples. Results of 18 probes for 6 DR loci and 5 standard probes are shown. Each dot represents the mean of triplicates. Dashed line indicates the cut-off value, the lowest MFI among 5 standard probes (MFI = 837.5).
doi:10.1371/journal.pone.0109823.g004

Customization of oligoprobes to detect genetic diversity around K65

In 31 specimens without signals, the sequence around K65 was very diverse, especially at codons K65, K66 and K67 (Table 3). The nucleotide position of A2723G, A2747G and C2750T were frequent polymorphism for the wild type amino acid K65, K66 and D67, respectively. Fourteen specimens had a G2748A mutation that led to D67N, a thymidine analogue mutation [19]. Based on these results we synthesized 10 additional oligoprobes (Table 4).

The specificity of the newly added oligoprobes was confirmed by the plasmids carrying the mutation (data not shown). Customization of the assay decreased the number of specimens without signals from 31 to 6 (Fig. 5).

Discussion

We developed a PCR-SSOP-Luminex DR assay that can identify 6 clinically important DR mutations for NRTI and NNRTI in a single well. To simplify the development, we chose clade B virus and focused on the following mutations in the RT region: M41L, K65R, K70R, K103N, M184V and T215Y/F. We designed a series of capture probes according to the database of the Japanese patients. MFI from hybridization with the corresponding probes was greater than 20-fold signal-to-noise ratio in plasmid experiments (Fig. 2), at least 2-fold signal-to-noise ratio using clinical samples (Fig. 4). The initial positive reaction was as low as 58.1% (43/74) in the highly polymorphic K65 region. The use of additional probes designed to match sequences in the patients' specimens improved the detection rate to 91.9% (68/74), demonstrating that the PCR-SSOP-Luminex assay can be customized to reflect sequences of the viruses prevalent in a given environment.

Transmission of viral strains with major DR mutations can reduce the efficacy of first-line regimens. Since the first report of a horizontal transmission of HIV-1 harboring a zidovudine-resistant mutation [20], 5% to 15% of treatment-naïve, HIV-1-infected individuals harbored the viruses with DR mutations in early 2000s in resource-rich settings [21–24]. It was suggested that transmission of drug resistance in the resource-rich settings can remain stable and at a low level [25]. However, in Japan where the transmission of drug-resistant viruses has historically been low, there seems to be an increasing trend [18,26]. Rates of transmitted HIV drug resistance has remained limited also in resource-limited settings (http://www.who.int/hiv/topics/drugresistance/en/), however, limitation on the first line and subsequent regimens would be a concern. Continued surveillance of drug resistant HIV-1 is warranted.

There are some multiplex strategies to detect the single-nucleotide differences, LigAmp assay [27,28], Nanostring assays [29], oligonucleotide ligation assay-based DNA chip [30], AS-PCR [31,32]. These assays provide substantial improvements in their detection sensitivity over conventional sequencing-based assays, however major limitation of these assays could be detecting one or few DR mutations at a time. PCR-SSOP-Liminex assay should be able to accommodate more DR mutations than the others.

One limitation of PCR-SSOP-Luminex assay is the assay sensitivity caused by diversity of HIV. We were able to detect DR mutations that constituted 10% of the mixture in the isogenic system using plasmids. Even after successful amplification, we could not get signal in considerable number of patient's specimens. By comparison with cloning and sequencing, we estimate that at least 20% mutant was necessary in the patient's specimens to be detected by the PCR-SSOP-Luminex assay. The sensitivity of detection by Sanger sequencing has been reported to be ~20% [33,34]. Sanger sequencing and PCR-SSOP-Luminex had approximately the same detection sensitivity on patient materials. In Sanger sequencing, nucleotide sequences are determined by the wave height. When the virus in the plasma is a mixture of the wild type and a mutant, each nucleotide is displayed as two waves in the same locus with different height according to the fraction in the sample. In the case of PCR-SSOP-Luminex, the wild type or mutant nucleotides are detected independently by the signal bound to the proper probes. Therefore, as we showed partly in this paper, the mutant detection by PCR-SSOP-Luminex assay could

Table 3. Sequence diversity around K65 in the 31 specimens.

Amino acid (HXB2-wt)	I63 K64 K65 K66 D67 S68	
Nucleotide (HXB2-wt)	**ATA AAG AAA AAA GAC AGT**	**Number of specimens**
	2747	
K66K-AAG	--- --- --- —G --- —	10
	2747 2748	
K66K-AAG/D67N-AAC	--- --- --- —G A— —	5
	2748	
D67N-AAC	--- --- --- --- A— —	3
	2750	
D67D-GAT	--- --- --- --- —T —	1
	2748	
K65K-AAG/D67N-AAC	--- --- —G --- A— —	2
	2748	
K65K-AAR/D67N-AAC	--- --- —R --- A— —[a]	1
	2747 2748	
K65K-AAG/K66K-AAG/D67N-AAC	--- --- —G —G A— —	1
	2741 2748	
K65K-AAG/D67N-AAC/K64K-AAA	--- —A —G --- A— —	1
	2747 2750	
K66K-AAG/D67D-GAT	--- --- --- —G —T —	1
	2748 2750	
D67N-AAT	--- --- --- --- A-T —	1
	2750 2751	
D67D-GAT/S68G-GGT	--- --- --- --- —T G-	2
	2747	
K65R-AGA/K66K-AAG	--- --- -G- —G --- —	1
	2750	
K65R-AGA/D67D-GAT	--- --- -G- --- —T —	2

[a]R: Mixed base of A and G.

doi:10.1371/journal.pone.0109823.t003

be improved by further customization to the circulating viruses. In our paper, we used maximum 23 oligoprobes in one tube or well. The evaluation of assay volume etc. would be necessary to determine actually possible maximum number of ologibrobes in

Table 4. Design of additional oligoprobes based on clinical samples.

Locus	Name of probe	Oligoprobes	Nucleotide sequence (5'-3')
K65			ATA AAG AAA AAA GAC AGT ACT
	K66K-AAG	ATAAAGAAAAAGGACAG	--- --- --- —G --- —
	K65R-AGA/K66K-AAG	ATAAAGAGAAAGGACAG	--- --- -G- —G --- —
	K66K-AAG/D67N-AAC	ATAAAGAAAAAGAACAG	--- --- --- —G A— ---
	K65R-AGA/K66K-AAG/D67N-AAC	ATAAAGAGAAAGAACAG	--- --- -G- —G A— —
	D67N-AAC	ATAAAGAAAAAAAACAGT	--- --- --- --- A— ---
	K65R-AGA/D67N-AAC	ATAAAGAGAAAAAACAG	--- --- -G- --- A— ---
	D67D-GAT	ATAAAGAAAAAGATAGT	--- --- --- --- —T ---
	K65R-AGA/D67D-GAT	ATAAAGAGAAAGATAGT	--- --- -G- --- —T ---
	K65K-AAG	ATAAAGAAGAAAGACAG	--- --- —G --- --- —
	K65K-AAG/D67N-AAC	ATAAAGAAGAAAAACAGTA	--- --- —G --- A— --- -

doi:10.1371/journal.pone.0109823.t004

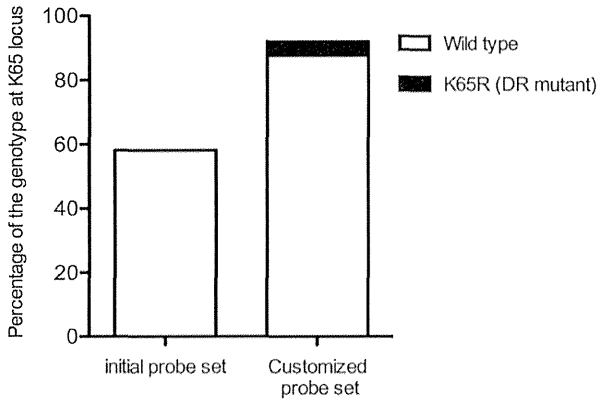

Figure 5. Improvement of the detection by the additional probes at K65 locus. The ordinate shows the percentage of the genotype at K65 locus determined by the PCR-SSOP-Luminex DR assay. One hundred % is the sample number (74) successfully amplified by PCR.
doi:10.1371/journal.pone.0109823.g005

one tube. 100 color-coded beads are available, theoretically, 100 probes could be applied (http://www.luminexcorp.com/Products/Instruments/Luminex100200/). Since the wild type or mutant nucleotides are detected as the signal of hybridized probes for each in the PCR-SSOP-Luminex assay, inclusion of multiplex probes based on the codon usages for the DR mutations and the sequence variations in the flanking region of circulating viruses would improve the detection. According to our results, we could develop, validate and customized PCR-SSOP-Luminex assay for detecting DR mutations at six positions in HIV-1 RT gene. The study numbers are very limited and we worked only on subtype B HIV-1 in this article. HIV-1 diversity is notoriously huge and sequences in an individual could be more diverse than acutely expanding viruses in the field [35]. Diagnostic use in individual patients is far from the actual application at present. We believe the assay would be more suitable for molecular epidemiological studies detecting regional trends of HIV-1 DR mutation over time.

PCR-SSOP-Luminex assay were widely used for the detection of papillomavirus, influenza surveillance etc. in developing countries [36,37]. Furthermore, application of Luminex technology to other pathogen (*C. difficile*, *Norovirus*, *E. coli* or *Salmonella*, *Rotavirus A*, *Campylobacter*, *Shigella* etc.) were reported recently [38]. It would be feasible to expect that the use of Luminex technology will be wide-spread in the near future. Furthermore, the application of PCR-SSOP-Luminex DR assay to non-clade B HIV-1 is currently under development. Future studies include refinement of the assay for use with specimens co-infected with HIV-1 and HBV.

Conclusions

We have developed a rapid high-throughput assay for DR testing. The assay can be customized by adding oligoprobes suitable for the circulating viruses. The assay may turn out to be a useful method especially for public health research in both resource-rich and resource-limited settings.

Acknowledgments

The authors thank Dr. Barbara Rutledge for discussion and editing English.

Author Contributions

Conceived and designed the experiments: LG NH AKT AI. Performed the experiments: LG NH AKT. Analyzed the data: LG NH TS WS. Contributed reagents/materials/analysis tools: MM. Contributed to the writing of the manuscript: LG NH AI. Provided clinical information and patient care: HN MK TK EA TK AI. Discussion: TI GFG.

References

1. Palella FJ Jr, Delaney KM, Moorman AC, Loveless MO, Fuhrer J, et al. (1998) Declining morbidity and mortality among patients with advanced human immunodeficiency virus infection. HIV Outpatient Study Investigators. N Engl J Med 338: 853–860.
2. Samji H, Cescon A, Hogg RS, Modur SP, Althoff KN, et al. (2013) Closing the Gap: Increases in Life Expectancy among Treated HIV-Positive Individuals in the United States and Canada. PLoS One 8: e81355.
3. Frentz D, Boucher CA, van de Vijver DA (2012) Temporal changes in the epidemiology of transmission of drug-resistant HIV-1 across the world. AIDS Rev 14: 17–27.
4. WHO (2012) WHO HIV Drug Resistance Report 2012. WHO Press.
5. WHO (2013) Consolidated guidelines on the use of antiretroviral drugs for treating and preventing HIV infection: Recommendations for a public health approach. WHO Press.
6. Sungkanuparph S, Techasathit W, Utaipiboon C, Chasombat S, Bhakeecheep S, et al. (2010) Thai national guidelines for antiretroviral therapy in HIV-1 infected adults and adolescents 2010. Asian Biomedicine 4: 515–528.
7. Clavel F, Hance AJ (2004) HIV drug resistance. N Engl J Med 350: 1023–1035.
8. Wainberg MA, Friedland G (1998) Public health implications of antiretroviral therapy and HIV drug resistance. Jama 279: 1977–1983.
9. Shafer RW, Rhee SY, Pillay D, Miller V, Sandstrom P, et al. (2007) HIV-1 protease and reverse transcriptase mutations for drug resistance surveillance. Aids 21: 215–223.
10. Balajee SA, Sigler L, Brandt ME (2007) DNA and the classical way: identification of medically important molds in the 21st century. Med Mycol 45: 475–490.
11. Dunbar SA (2006) Applications of Luminex xMAP technology for rapid, high-throughput multiplexed nucleic acid detection. Clin Chim Acta 363: 71–82.
12. Itoh Y, Mizuki N, Shimada T, Azuma F, Itakura M, et al. (2005) High-throughput DNA typing of HLA-A, -B, -C, and -DRB1 loci by a PCR-SSOP-Luminex method in the Japanese population. Immunogenetics 57: 717–729.
13. Wensing AM, Calvez V, Gunthard HF, Johnson VA, Paredes R, et al. (2014) 2014 update of the drug resistance mutations in HIV-1. Top Antivir Med 22: 642–650.
14. Cheng-Mayer C, Quiroga M, Tung JW, Dina D, Levy JA (1990) Viral determinants of human immunodeficiency virus type 1 T-cell or macrophage tropism, cytopathogenicity, and CD4 antigen modulation. J Virol 64: 4390–4398.
15. Shioda T, Levy JA, Cheng-Mayer C (1991) Macrophage and T cell-line tropisms of HIV-1 are determined by specific regions of the envelope gp120 gene. Nature 349: 167–169.
16. Ho SN, Hunt HD, Horton RM, Pullen JK, Pease LR (1989) Site-directed mutagenesis by overlap extension using the polymerase chain reaction. Gene 77: 51–59.
17. Koga I, Odawara T, Matsuda M, Sugiura W, Goto M, et al. (2006) Analysis of HIV-1 sequences before and after co-infecting syphilis. Microbes Infect 8: 2872–2879.
18. Hattori J, Shiino T, Gatanaga H, Yoshida S, Watanabe D, et al. (2010) Trends in transmitted drug-resistant HIV-1 and demographic characteristics of newly diagnosed patients: nationwide surveillance from 2003 to 2008 in Japan. Antiviral Res 88: 72–79.
19. Johnson VA, Calvez V, Gunthard HF, Paredes R, Pillay D, et al. (2013) Update of the drug resistance mutations in HIV-1: March 2013. Top Antivir Med 21: 6–14.
20. Erice A, Mayers DL, Strike DG, Sannerud KJ, McCutchan FE, et al. (1993) Brief report: primary infection with zidovudine-resistant human immunodeficiency virus type 1. N Engl J Med 328: 1163–1165.
21. Cane P, Chrystie I, Dunn D, Evans B, Geretti AM, et al. (2005) Time trends in primary resistance to HIV drugs in the United Kingdom: multicentre observational study. Bmj 331: 1368.
22. Descamps D, Chaix ML, Andre P, Brodard V, Cottalorda J, et al. (2005) French national sentinel survey of antiretroviral drug resistance in patients with HIV-1 primary infection and in antiretroviral-naive chronically infected patients in 2001–2002. J Acquir Immune Defic Syndr 38: 545–552.

23. Weinstock HS, Zaidi I, Heneine W, Bennett D, Garcia-Lerma JG, et al. (2004) The epidemiology of antiretroviral drug resistance among drug-naive HIV-1-infected persons in 10 US cities. J Infect Dis 189: 2174–2180.
24. Wensing AM, van de Vijver DA, Angarano G, Asjo B, Balotta C, et al. (2005) Prevalence of drug-resistant HIV-1 variants in untreated individuals in Europe: implications for clinical management. J Infect Dis 192: 958–966.
25. Yerly S, von Wyl V, Ledergerber B, Boni J, Schupbach J, et al. (2007) Transmission of HIV-1 drug resistance in Switzerland: a 10-year molecular epidemiology survey. Aids 21: 2223–2229.
26. Gatanaga H, Ibe S, Matsuda M, Yoshida S, Asagi T, et al. (2007) Drug-resistant HIV-1 prevalence in patients newly diagnosed with HIV/AIDS in Japan. Antiviral Res 75: 75–82.
27. Shi C, Eshleman SH, Jones D, Fukushima N, Hua L, et al. (2004) LigAmp for sensitive detection of single-nucleotide differences. Nat Methods 1: 141–147.
28. Church JD, Towler WI, Hoover DR, Hudelson SE, Kumwenda N, et al. (2008) Comparison of LigAmp and an ASPCR assay for detection and quantification of K103N-containing HIV variants. AIDS Res Hum Retroviruses 24: 595–605.
29. Geiss GK, Bumgarner RE, Birditt B, Dahl T, Dowidar N, et al. (2008) Direct multiplexed measurement of gene expression with color-coded probe pairs. Nat Biotechnol 26: 317–325.
30. Deng JY, Zhang XE, Mang Y, Zhang ZP, Zhou YF, et al. (2004) Oligonucleotide ligation assay-based DNA chip for multiplex detection of single nucleotide polymorphism. Biosens Bioelectron 19: 1277–1283.
31. Boltz VF, Ambrose Z, Kearney MF, Shao W, Kewalramani VN, et al. (2012) Ultrasensitive allele-specific PCR reveals rare preexisting drug-resistant variants and a large replicating virus population in macaques infected with a simian immunodeficiency virus containing human immunodeficiency virus reverse transcriptase. J Virol 86: 12525–12530.
32. Rowley CF, Boutwell CL, Lockman S, Essex M (2008) Improvement in allele-specific PCR assay with the use of polymorphism-specific primers for the analysis of minor variant drug resistance in HIV-1 subtype C. J Virol Methods 149: 69–75.
33. Zagordi O, Klein R, Daumer M, Beerenwinkel N (2010) Error correction of next-generation sequencing data and reliable estimation of HIV quasispecies. Nucleic Acids Res 38: 7400–7409.
34. Mohamed S, Ravet S, Camus C, Khiri H, Olive D, et al. (2014) Clinical and analytical relevance of NNRTIs minority mutations on viral failure in HIV-1 infected patients. J Med Virol 86: 394–403.
35. Walker BD, Korber BT (2001) Immune control of HIV: the obstacles of HLA and viral diversity. Nat Immunol 2: 473–475.
36. Jiang HL, Zhu HH, Zhou LF, Chen F, Chen Z (2006) Genotyping of human papillomavirus in cervical lesions by L1 consensus PCR and the Luminex xMAP system. J Med Microbiol 55: 715–720.
37. Vongphrachanh P, Simmerman JM, Phonekeo D, Pansayavong V, Sisouk T, et al. (2010) An early report from newly established laboratory-based influenza surveillance in Lao PDR. Influenza Other Respir Viruses 4: 47–52.
38. Claas EC, Burnham CA, Mazzulli T, Templeton K, Topin F (2013) Performance of the xTAG(R) gastrointestinal pathogen panel, a multiplex molecular assay for simultaneous detection of bacterial, viral, and parasitic causes of infectious gastroenteritis. J Microbiol Biotechnol 23: 1041–1045.

RETROVIROLOGY

RESEARCH Open Access

Switching and emergence of CTL epitopes in HIV-1 infection

Chungyong Han[1,10], Ai Kawana-Tachikawa[1], Akihisa Shimizu[1], Dayong Zhu[1], Hitomi Nakamura[2,3], Eisuke Adachi[3], Tadashi Kikuchi[1,3], Michiko Koga[1], Tomohiko Koibuchi[3], George F Gao[4], Yusuke Sato[5,6], Atsushi Yamagata[5,6], Eric Martin[7,8], Shuya Fukai[5,6], Zabrina L Brumme[7,8] and Aikichi Iwamoto[1,2,3,9*]

Abstract

Background: Human Leukocyte Antigen (HLA) class I restricted Cytotoxic T Lymphocytes (CTLs) exert substantial evolutionary pressure on HIV-1, as evidenced by the reproducible selection of HLA-restricted immune escape mutations in the viral genome. An escape mutation from tyrosine to phenylalanine at the 135th amino acid (Y135F) of the HIV-1 *nef* gene is frequently observed in patients with HLA-A*24:02, an HLA Class I allele expressed in ~70% of Japanese persons. The selection of CTL escape mutations could theoretically result in the *de novo* creation of novel epitopes, however, the extent to which such dynamic "CTL epitope switching" occurs in HIV-1 remains incompletely known.

Results: Two overlapping epitopes in HIV-1 *nef*, Nef126-10 and Nef134-10, elicit the most frequent CTL responses restricted by HLA-A*24:02. Thirty-five of 46 (76%) HLA-A*24:02-positive patients harbored the Y135F mutation in their plasma HIV-1 RNA. Nef codon 135 plays a crucial role in both epitopes, as it represents the C-terminal anchor for Nef126-10 and the N-terminal anchor for Nef134-10. While the majority of patients with 135F exhibited CTL responses to Nef126-10, none harboring the "wild-type" (global HIV-1 subtype B consensus) Y135 did so, suggesting that Nef126-10 is not efficiently presented in persons harboring Y135. Consistent with this, peptide binding and limiting dilution experiments confirmed F, but not Y, as a suitable C-terminal anchor for HLA-A*24:02. Moreover, experiments utilizing antigen specific CTL clones to recognize endogenously-expressed peptides with or without Y135F indicated that this mutation disrupted the antigen expression of Nef134-10. Critically, the selection of Y135F also launched the expression of Nef126-10, indicating that the latter epitope is created as a result of escape within the former.

Conclusions: Our data represent the first example of the *de novo* creation of a novel overlapping CTL epitope as a direct result of HLA-driven immune escape in a neighboring epitope. The robust targeting of Nef126-10 following transmission (or *in vivo* selection) of HIV-1 containing Y135F may explain in part the previously reported stable plasma viral loads over time in the Japanese population, despite the high prevalence of both HLA-A*24:02 and Nef-Y135F in circulating HIV-1 sequences.

Background

Cytotoxic T lymphocytes (CTLs) are key players in the immune control of Human Immunodeficiency Virus 1 (HIV-1), as they recognize virally-derived peptide epitopes presented by HLA class I molecules on the infected cell surface [1,2]. Over the course of infection however, HIV-1 mutations arise within the infected individual, notably in targeted CTL epitopes, that allow the virus to escape immune recognition by CTLs. Importantly, despite the hypermutability of HIV-1, these immune escape mutations often arise in a stereotypical manner [3,4] that is highly predictable based on the specific HLA class I molecules expressed by the host [5-8]. Although selection of HLA-associated mutations in HIV-1 is driven by immune pressure, these amino acid substitutions sometimes result in the induction of a *de novo* immune response in which the mutant epitope is recognized by a TCR associated with a different CTL subset [7,9]. What is less well-characterized is the

* Correspondence: aikichi@ra3.so-net.ne.jp
[1]Division of Infectious Diseases, Advanced Clinical Research Center, the Institute of Medical Science, the University of Tokyo, 4-6-1 Shirokanedai, Minato-ku, Tokyo 108-8639, Japan
[2]Department of Infectious Disease Control, the International Research Center for Infectious Diseases, the Institute of Medical Science, the University of Tokyo, Tokyo, Japan
Full list of author information is available at the end of the article